Assessing atoll island physical robustness: application to Rangiroa Atoll, French Polynesia

Virginie Duvat, Natacha Volto, Stéphane Costa, Olivier Maquaire, Cécilia Pignon-Mussaud, Robert Davidson

Version of Record: https://www.sciencedirect.com/science/article/pii/S0169555X21002798
Manuscript_7e696567e2a0692b81b52371c84d9939

Assessing atoll island physical robustness: application to Rangiroa Atoll, French Polynesia

Virginie Duvat[1], Natacha Volto[1], Stéphane Costa[2], Olivier Maquaire[2], Cécilia Pignon-Mussaud[1], Robert Davidson[2]

[1]UMR LIENSs, La Rochelle-University-CNRS, 17000 La Rochelle, France

[2]Normandie Univ, Unicaen, CNRS, LETG, 14000 Caen, France

Corresponding author: virginie.duvat@univ-lr.fr

1. Introduction

Atoll islands are recently-formed (generally < 4,000 yr BP) and low-lying (generally < 3 m) islands composed of biologically derived carbonate sand, gravel and boulders, resting on circular reef structures at or near contemporary sea level and often encircling a central lagoon (Woodroffe, 2008; McLean, 2011; Gischler, 2016). These islands host relatively large populations in some countries and territories of the Indian and Pacific Oceans, including the Maldives (530,953 inhabitants), Kiribati (117,646 inhabitants), the Federated States of Micronesia (113,815 inhabitants), the Marshall Islands (58,791 inhabitants), French Polynesia (15,544 inhabitants) and Tuvalu (11,646 inhabitants). Because of their physical configuration, atoll countries and territories are among the territories that are the most threatened by climate variability and climate change impacts, including especially the combination of gradual sea-level rise (SLR) and increased storm wave heights, and the degradation of coral reefs under both ocean warming and acidification and increased human disturbances (Bindoff et al., 2019; Cornwall et al., 2021; Duvat et al., 2021; Gattuso et al., 2015; Hoeke et al., 2021; Kane and Fletcher, 2020; Mentaschi et al., 2017; Oppenheimer et al., 2019; Perry et al., 2018; Vitousek et al., 2017).

Physical assessments of risks to atoll island habitability under climate change have investigated the risks of island erosion (Beetham et al., 2017; Beetham and Kench, 2018; Shope et al., 2017; Shope and Storlazzi, 2019; Tuck et al., 2019) and temporary or permanent submergence (Giardino et al., 2018; Owen et al., 2016; Storlazzi et al., 2018). These studies have mainly considered two types of parameters, namely island elevation (which influences marine flooding) and island capacity to naturally adjust to climate-ocean changes through sediment reorganization, that is, changes in position, shape, volume and elevation (which allow for an island to persist). Such studies agree that atoll islands will likely experience increased physical destabilization over the second half of the 21st century as a result of

increased marine flooding and shoreline instability, with potential decreases in shoreline elevation, island width and volume, whatever the climate scenario. Beyond these key findings, these studies have limitations. First, they are based on idealized islands that do not reflect the high diversity of atoll island configurations, although recognized by previous studies (e.g. Nurse et al., 2014; Richmond, 1992; Stoddart and Steers, 1977; Woodroffe, 2008). Second, they used models that neglect some variables driving island change, including the response of ecosystems (especially the reef ecosystem and island vegetation) and sediment transport, notably cross-shore and overwash-driven. Third, they overlooked the specific situation of inhabited islands exhibiting a decreased capacity to adjust to climate-ocean changes, as a result of the obstruction of sediment transport pathways and reduction of coastal accommodation space by human developments (Duvat, 2019; Duvat and Magnan, 2019; Duvat et al., 2020a; McLean and Kench, 2015; Schuerch et al., 2018).

Because atoll islands exhibit diverse physical (Richmond, 1992; Stoddart and Steers, 1977; Woodroffe, 2008) and human (Duvat and Magnan, 2019; McLean and Kench, 2015) configurations, which together influence their current and future habitability (Duvat et al., 2021; Magnan et al., 2019), the present article proposes a more comprehensive assessment of their 'physical robustness' that considers not only geomorphic, but also ecological and human determinants of this robustness. 'Physical robustness' refers to the ability of an atoll island to both resist to extreme events (i.e. 'absorb a disturbance with minimal alteration'; Masselink and Lazarus, 2019, p. 5), and naturally adjust (i.e. its size, shape, elevation, volume and position) to any changes in boundary conditions through sediment reworking (McLean, and Kench, 2015; Tuck et al., 2019). Using a sample of twelve islands that are considered key by the local population and public authorities to the maintenance of the habitability of Rangiroa Atoll (Tuamotu Archipelago, French Polynesia) in the future, and that exhibit contrasting physical configurations, we assess atoll island physical robustness using six parameters: (1)

island size; (2) island elevation; (3) island shape; (4) island structure; (5) island vegetation; and (6) the influence of local human activities on island dynamics and natural capacity to adjust to climate-ocean changes.

2. Study area

The Tuamotu Archipelago is one of the five archipelagos composing French Polynesia (Figure 1A), and the largest group of atolls in the world. It consists of seventy-seven atolls stretching > 1500 km from northwest to southeast and extending from 14°21'S to 23°22'S and from 134°28'W to 148°43'W. This study focuses on Rangiroa, which is the largest atoll in the archipelago, with maximal dimensions of 79 by 32 km (Figure 1B), and a total landmass of approximately 66 km^2 (Andrefouët et al., 2008) made of around 240 islands (Stoddart, 1969). The atoll has two deep passes in the north (Avatoru and Tiputa passes), having a depth of between 31 and 34 m (Figure 1B). It is the most populated atoll of the Tuamotu chain, with a population of 2,567 inhabitants (ISPF, 2017). This study examines twelve islands of the atoll, including the ten northern islands concentrating the population and infrastructure (numbered from 1 to 10 from west to east in this study) and two 'outer' islands respectively located at its north-western (island 11) and southern (island 12) ends (Figures 1B and 2).

The islands of Rangiroa Atoll have accreted on a conglomerate platform inherited from a sea level ~ +0.60 m higher than Present from around 2500 to 1000 years BP (Montaggioni et al., 2021). With the exception of island No.7, which is a recently-formed rim-perpendicular elongated islet, these islands are typical 'motus' (Stoddart, 1969; Stoddart and Steers, 1977; Richmond, 1992; Woodroffe, 2008), exhibiting an ocean-facing elevated beach ridge composed of coarse material (coral shingle, rubble or blocks) and a less prominent lagoon-facing sandy beach. Islands 1, 2 and 11 exhibit low-lying swampy areas in their interior. Islands Nos. 1 and 2 and islands Nos. 8 and 9 are separated by Avatoru and Tiputa passes,

respectively, whereas the other islands are separated by inter-islet channels, i.e. ‘hoa’ (Kench and McLean, 2004). Between 1966 and 2013, islands Nos. 2 to 6, 8 and 9 were stable in area, while island No.7 formed (Duvat et al., 2017a). These inhabited and developed islands, especially islands Nos. 2 to 9, show widespread local human disturbances, including in particular lagoon-side land reclamation, extensive aggregate extraction from beaches, longitudinal and transversal coastal protection structures, and harbors. As a result, they exhibit partly hardened shoreline (5.45% to 36.39% of fixed shoreline), modified coastal dynamics, and human-induced erosion and beach loss (see e.g. Figure 3 in Duvat et al., 2020a).

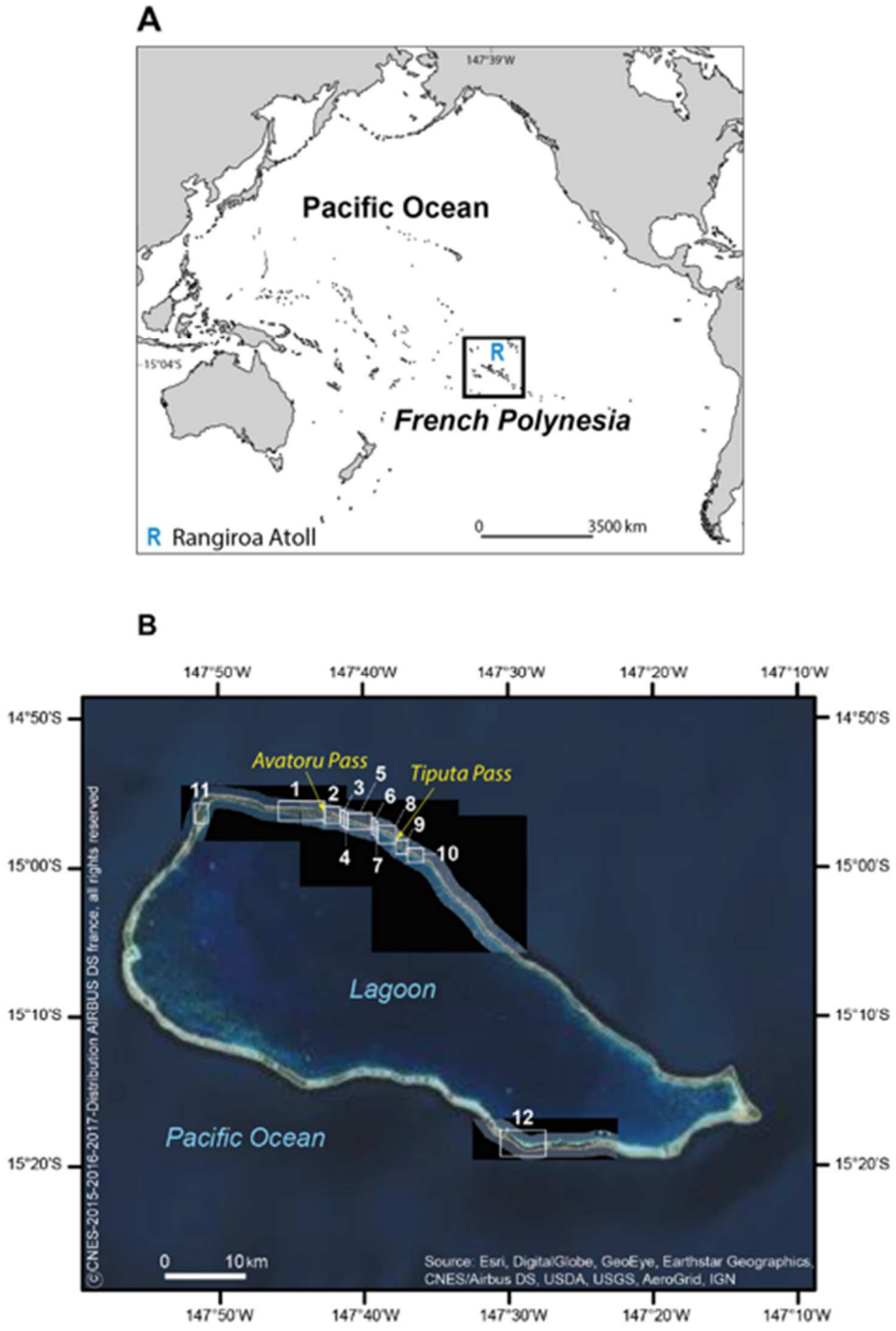

Figure 1. Location map of the study area.

Panel A shows the location of the Tuamotu atolls (represented by a square) in French Polynesia and of Rangiroa Atoll in the northern part of the chain. On Panel B, the location of study islands is indicated in white, using Arabic numeral (same island numbers used throughout the manuscript), and the location of the two passes of the atoll is shown in yellow.

Figure 2. Study islands.
See location in Figure 1B. The precise location and boundaries (white line) of each island are shown.

The climate of the study area is controlled by the combined influence of trade winds from the northeast to southeast, which are the strongest during the Austral winter (April-October), and of tropical and extra-tropical storms respectively occurring during the Austral summer (November-March) and Austral winter (April-October) (Andrefouët et al., 2012). Tropical cyclones (TCs) rarely affect Rangiroa Atoll. The most intense TCs that passed over this atoll

over the last century were category 3 TCs Orama (22-27 February 1983) and Veena (9-12 April 1983). The most influential swells from a geomorphic perspective are those generated by the trade winds, moderate tropical lows (Duvat et al., 2020b) and distant-source southern storms, including the intense event of 19-22 July 1996 as well as two to three low to moderate events each year according to inhabitants. The 1983 TCs and 1996 southern swell predominantly had erosive effects on islands Nos. 2 to 9 (Duvat et al., 2017a). Astronomical tides are micro-tidal and semi-diurnal. The mean and maximum (i.e. for the highest spring tides) tidal ranges are of 0.5 m and 0.6 m, respectively (Pirazzoli and Montaggioni, 1986; SHOM, 2016). In the study area, Mean Sea Level is 0.39 m above hydrographic zero, which corresponds to the lowest spring tide (Figure 3). Storm surges associated with TCs can have amplitudes of the order of 1.0 m, as during TC Orama in 1983 (Des Garets, 2005). Numerical modelling revealed that extreme water levels under the influence of cyclonic swells (Hs: 8 m to 12 m) respectively reach up to 4.5 m and 2.1 m above hydrographic zero on the ocean (Pedreros et al., 2010) and lagoon (Damlamian and Kruger, 2013) coasts of Avatoru Island, northern part of the atoll. Under these water levels, the northern islands of Rangiroa Atoll, which are the most exposed to TCs as a result of north/south or north-western/south-eastern cyclone tracks (Larrue and Chiron, 2010), flood (Magnan et al., 2018). Estimated absolute SLR between 1950 and 2009 was 2.5 mm ± 0.5 mm/y, i.e. higher than the global mean SLR for the twentieth century, estimated to be ~1.8 mm/y by Church and White (2011) and 1.2 ± 0.2 mm/y by Hay et al. (2015).

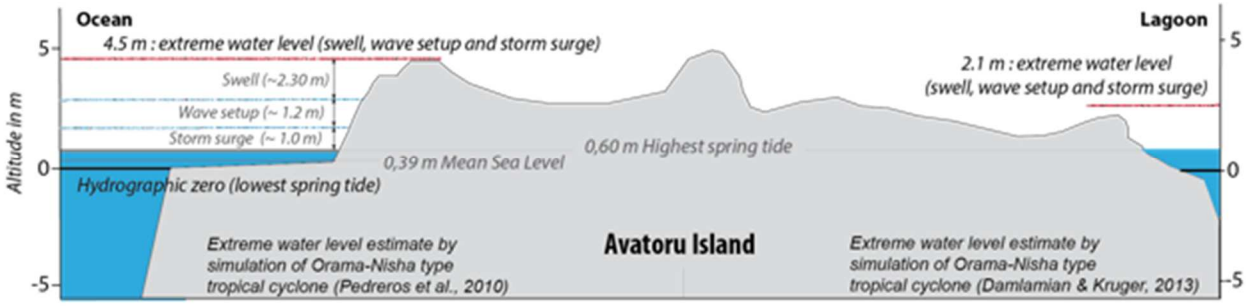

Figure 3. Extreme water levels associated with an Orama-Nisha type Tropical Cyclone on Avatoru Island, Rangiroa Atoll.

This figure uses the results of two available flood modelling studies to illustrate extreme water levels on the ocean (where the island floods at 4.50 m) and lagoon (where it floods at 2.1 m) coasts of the most populous island of Rangiroa Atoll, compared to MSL and the lowest spring tide.

3. Materials and methods

3.1. Justification of island sample

The main objective of this study is to assess the physical robustness of twelve islands that are considered key by the local population and public authorities to the maintenance of the atoll's habitability because they are already settled, cultivated or targeted for future development. These islands constitute a relevant island sample to assess atoll island physical robustness because they are geomorphologically (in terms of size, geomorphic features, shape and elevation) and ecologically diverse, representative of the types of islands found on the atoll, and unequally affected by local human disturbances. The island sample includes both the settled islands of the atoll concentrating most of the population and infrastructure (Nos. 2 to 9) and some peripheral islands used for agricultural purposes, some of which are settled (Nos. 1, 10) whereas others are not (Nos. 11 and 12). These twelve islands allow to interrogate the variability of island physical robustness across Rangiroa Atoll.

3.2. Data sources

3.2.1. Satellite imagery

High resolution (2013, 2015, 2016 and 2017) Pléiades satellite images obtained from Airbus Defence and Space archives are used in this study (Table 1). The resolution of these images was of 2 m and 0.50 m for multispectral (XS) and panchromatic (P) images, respectively. These images were pansharpened using Gram Schmidt Cubic Convolution Pan-sharpening algorithm (ENVI software version 5.4; Laben and Brower, 2000) to generate a color image having a spatial resolution of 0.50 m which was used for data generation. This resolution is appropriate for geomorphic (e.g. shoreline change assessment; Duvat et al., 2017a; Holdaway and Ford, 2018; Mann and Westphal, 2014; Purkis et al., 2016) and ecological (e.g. island vegetation) analysis (see e.g. Ellison et al., 2017). These images were used to generate island size and to analyze island shape, structure and vegetation.

Table 1. Characteristics of the satellite images used in this study.

XS: multispectral; P: panchromatic.

Date (day/month/year)	Sensor	Pixel size (m)	Islands covered
01/10/2013	Pléiades 1A XS	2	1-10
01/10/2013	Pléiades 1A P	0.5	1-10
20/02/2015	Pléiades 1B XS	2	12
20/02/2015	Pléiades 1B P	0.5	12
16/10/2016	Pléiades 1A XS	2	1-3, 11
16/10/2016	Pléiades 1A P	0.5	1-3, 11
16/10/2016	Pléiades 1A XS	2	1-10
16/10/2016	Pléiades 1A P	0.5	1-10
15/01/2017	Pléiades 1B XS	2	5-10
15/01/2017	Pléiades 1B P	0.5	5-10

3.2.2. Fieldwork

Over the 2013-2018 period, regular fieldwork was conducted by the authors on inhabited islands Nos. 2 to 9, which allowed documenting island structure, which relates to the morphological features of an island (section 3.3.4); island vegetation (section 3.3.5); and the

nature, location and spatial extent of human disturbances liable to altering natural dynamics (section 3.3.6). In May 2018, a one-week field trip was conducted on islands Nos. 1 and 10 (inhabited), 11 (uninhabited), and 12 (cultivated but non-permanently inhabited) to document the abovementioned variables and island elevation (section 3.3.2).

3.3. Methodology

Kumar et al. (2018) used four variables to assess island susceptibility to coastal erosion under climate change, including lithology (based on the distinction between continental and volcanic and reef islands), circularity (using the roundness index), height (using island maximum elevation) and land area. Based on this previous study and on a recent review of available literature (see 2.1.1 and 3.2.1 in Duvat et al., 2021), we identified six main variables influencing atoll island physical robustness under climate variability and change: island size, elevation, shape, structure, vegetation, and the influence of human activities on island capacity to naturally adjust to climate-ocean changes. A synthetic presentation of the methodology (variables and sub-variables, their definition, their justification and the classes used) is available in Supplementary Material 1.

3.3.1. Variable 1: Island size

Island size (measured in hectares) influences island susceptibility to be physically destabilized by storm events and gradual SLR through enhanced coastal erosion and marine flooding causing changes to island position and configuration (e.g. breaking up) which may eventually lead to island disappearance. Large islands are more likely to persist both in the face of extreme events such as TCs and under slow onset changes such as SLR compared to small islands (Aslam and Kench, 2017; Duvat et al., 2017a and 2017b; Duvat, 2019; McLean and Kench, 2015; Woodroffe, 1983). Small islands are more susceptible to be washed away by storm events (see e.g. in Tikehau Atoll in Duvat, 2019) and to undergo contraction and eventually disappearance under contemporary SLR (see e.g. in the Solomon Islands in Albert

et al., 2016; and in New Caledonia in Garcin et al., 2016). Additionally, large islands are more likely to have flood-safe interiors in the face of extreme climate events, whereas small islands may exhibit flooding over most or the entirety of their surface (see Magnan et al., 2018 for examples on Rangiroa Atoll; and Duvat and Pillet, 2017 for the extent of cyclone-induced flooding on both small and large islands of Takapoto Atoll). Assuming that the larger the island, the less susceptible to physical destabilization by coastal erosion and/or marine flooding, we therefore use island size as a first proxy for island susceptibility to physical destabilization.

Current (i.e. estimated between 2013 and 2017, depending on islands; Table 1) island size was generated for each island using the stability line (i.e. the vegetation line or the outer limit of human constructions, such as buildings and engineered structures, depending on the context) as a shoreline proxy (see Duvat et al., 2017a for details). We distinguished between five classes: $x < 10$ ha (class 1); $10 \leq x < 50$ ha (class 2); $50 \leq x < 100$ ha (class 3); $100 \leq x < 200$ ha (class 4); $x \geq 200$ ha (class 5).

3.3.2. Variable 2: Island elevation

Island elevation determines the risk of island temporary and permanent submergence. Additionally, island elevation indirectly provides information on an island's volume, which was not calculated here due to data limitations. Because it comprises a limited volume of sediments, a very low-lying and small island is more susceptible to breaking up or washing away in the face of storm waves (e.g. Fig. 15a in Duvat, 2019) and to marine flooding compared to an elevated island composed of series of storm ridges and/or having high sand dunes. Island physical robustness is therefore assumed to be proportional to island elevation.

Based on this assumption, five criteria were used to assess island elevation:

(1) Averaged island elevation provides a general estimate of island elevation. It was obtained by averaging the elevation of all the points of a given across-island transect (i.e. averaged transect elevation), and then averaging the values obtained for all transects (i.e. averaged island elevation) for each island. Averaged island elevation includes all the highest elevated features, including sand dunes and storm ridges, and all the lowest features, such as inner depressions (e.g. swamps). The minimum and maximum elevation values obtained were used to determine the five classes (Table 2).

(2) Maximum ocean-side beach ridge elevation determines island susceptibility to be flooded by ocean waves during an extreme event (e.g. cyclone or distant-source waves). It corresponds to the highest point surveyed on the ocean-side beach ridge. This point was extracted from each transect and the highest points of all transects were averaged for each island. The minimum and maximum elevation values obtained were used to determine the five classes (Table 2).

(3) Maximum lagoon-side beach ridge elevation determines island susceptibility to be flooded as a result of extreme water levels affecting the lagoon. It corresponds to the highest point surveyed on the lagoon-side beach ridge. This point was extracted from each transect and the highest points of all transects were averaged for each island. The minimum and maximum elevation values obtained were used to determine the five classes (Table 2).

For (2) and (3), the obtained values are indicative of the risk of marine flooding through wave overtopping, which can occur on both the ocean and lagoon sides of islands (Canavesio, 2019; Duvat et al., 2018; Magnan et al., 2018). The higher the value, the lower the risk of marine flooding, and conversely.

(4) Lowest elevation in the inner part of the island is indicative of the risk of water accumulation in the island's interior. This risk is generated (i) by wave overtopping in the case of a low-lying ocean- or lagoon-side beach ridge or of beach ridge breaching, e.g. during

a storm, and (ii) by potential seawater ingress from below due to an increase in the level of the underlying fresh groundwater lens, especially during extreme sea levels associated with storms (Duvat et al., 2018). The lowest point was extracted from each transect and the lowest points of all transects were averaged for each island. The minimum and maximum elevation values obtained were used to determine the five classes (Table 2).

(5) The highest point is indicative of the ability of an island to have flood-safe inner areas during extreme water levels. This point can be located inland where inner storm ramparts or sand dunes occur or at beach ridges if they do not. In the former case, this point differs from the highest point extracted from beach ridges, while in the latter case it does not. In islands where taro is cultivated (which does not occur on study islands), the highest point can also correspond to mounds adjacent to taro pits. The highest point was extracted from each transect and the highest points of all transects were averaged for each island. The minimum and maximum elevation values obtained were used to determine the five classes (Table 2).

For each of these five criteria, we ranked from lowest to highest elevation using five classes (Table 2).

Table 2. Method used to assess atoll island elevation.

The five classes presented in this table were determined based on the minimum and maximum values obtained. Elevations are expressed in meters, using the hydrographic zero as a reference. Of note, available numerical modelling studies indicate that the northern settled island of Avatoru floods at extreme water levels of 4.5 m (above hydrographic zero) along its ocean coast (Pedreros et al., 2010) and of 2.1 m (above hydrographic zero) along its lagoon coast (Damlamian and Kruger, 2013) (Figure 3).

Averaged island elevation (m)	Score	Maximum ocean-side beach ridge elevation (m)	Score	Maximum lagoon-side beach ridge elevation (m)	Score	Lowest elevation in the inner part of the island (m)	Score	Highest point (m)	Score	Total
$x \leq 1.81$	1	$x \leq 3.99$	1	$x \leq 1.61$	1	$x \leq 1.13$	1	$x \leq 4.13$	1	5

$1.81 < x \leq 2.00$	2	$3.99 < x \leq 4.57$	2	$1.61 < x \leq 1.78$	2	$1.13 < x \leq 1.33$	2	$4.13 < x \leq 4.85$	2	10
$2.00 < x \leq 2.16$	3	$4.57 < x \leq 5.15$	3	$1.78 < x \leq 1.95$	3	$1.33 < x \leq 1.53$	3	$4.85 < x \leq 5.57$	3	15
$2.16 < x \leq 2.32$	4	$5.15 < x \leq 5.73$	4	$1.95 < x \leq 2.12$	4	$1.53 < x \leq 1.73$	4	$5.57 < x \leq 6.29$	4	20
$x > 2.32$	5	$x > 5.73$	5	$x > 2.12$	5	$x > 1.73$	5	$x > 6.29$	5	25

We then added the scores obtained for each criterion. Final scores ranging between 5 and 25 were classified as follows: $5 \leq x < 9$ (class 1); $9 \leq x < 13$ (class 2); $13 \leq x < 17$ (class 3); $17 \leq x < 21$ (class 4); $21 \leq x \leq 25$ (class 5).

For islands Nos. 2 to 9, we used high resolution across-island topographic transects collected in 2011 by the South Pacific Applied Geoscience Commission (SOPAC) using GPS in RTK (Real Time Kinematic) mode. We interpolated these topographic transects using the kriging interpolation method. In addition, elevation data were generated by topographic surveys on study islands Nos. 1 and 10 to 12. For all islands, survey transect lines are oriented perpendicular to the shoreline from the ocean reef flat to the lagoon reef flat, allowing to capture differences in island elevation (Supplementary Material 2). The topographic surveys conducted on islands Nos. 1 and 10 to 12 were undertaken in October 2016 and May 2018, using standard GNSS techniques (Trimble with a base station 5700 GNSS and a mobile receiver 5800 GNSS and R8s GNSS) in RTK mode with radio link (Supplementary Material 3). Three to six transect lines were generated for each island, depending on island length. In total, 43 transects were generated and analyzed (Supplementary Material 2).

3.3.3. Variable 3: Island shape

In line with Kumar et al. (2018), we used circularity as the shape measure. Circular islands are less susceptible to change in structure than irregular shaped islands because they have less impeded alongshore sediment movement. For example, elongated islands are more liable to change in position as a result of their migration on the reef platform (see e.g. Duvat, 2019; Ford and Kench, 2014, Figure 3B) than typical circular or triangular sand cays located at the confluence of multiple wave/current directions. Elongated islands may undergo major

changes in shape over both short periods of time as a result of cyclone-induced fragmentation and long periods of fair weather favorable to aggregation with nearby islands (see e.g. Spennemann (1996) on Majuro Atoll; Ford and Kench (2014) on Nadikdik Atoll; Duvat and Pillet (2017) on Takapoto Atoll). We therefore consider that island physical robustness is proportional to island circularity.

A circular island is one with the smallest possible perimeter for a given area, compared with an island that has promontories and bays, and therefore a longer coastline. We used the most recent (i.e. 2013 or 2016, depending on availability) stability line to generate island perimeter and land area. As in Kumar et al. (2018), circularity was calculated as a ratio of the shape of a circle to the shape of the island polygon, where shape equals perimeter (P) divided by the square root of the area (A). A circle has a shape factor of 3.54 ($P_{circle} / \sqrt{A_{circle}} = 2\pi r / \sqrt{(\pi r^2)} = 3.54$), with the circularity of an island calculated as $3.54/(P_{island} / \sqrt{A_{island}})$. If an island is perfectly circular, the ratio is 1. In contrast, the least circular islands have a ratio approaching 0. Considering that island physical robustness is proportional to island circularity, we then ranked from lowest to highest circularity, and therefore physical robustness, as follows: $x < 0.20$ (class 1); $0.20 \leq x < 0.40$ (class 2); $0.40 \leq x < 0.60$ (class 3); $0.60 \leq x < 0.80$ (class 4); $x \geq 0.80$ (class 5).

3.3.4. Variable 4: Island structure

Island structure relates to the morphological features of an island. Some features are known to be physically unstable, including sand and gravel spits, island tips, and shore-parallel and shore-perpendicular elongated low-lying areas, with the latter corresponding to ancient hoa that have been filled with sediments over time (Duvat, 2019). These features are susceptible to be physically destabilized, i.e. heavily eroded or washed away (see e.g. Duvat et al., 2017a), or flooded (e.g. Magnan et al., 2018), during storm events. Lagoon-side elongated swamps separated from the lagoon by narrow sand and gravel spits are liable to be connected

again with the lagoon during wave events through spit breaching, which would profoundly modify the lagoon side of concerned islands. These features therefore contribute to reducing an island's physical robustness. On the contrary, other features, such as lithified formations (e.g. conglomerate), are acknowledged to increase an island's physical stability and resistance to storm waves, thereby increasing its physical robustness in the face of climate pressures (Woodroffe, 2008; Montaggioni et al., 2021). Island features were inventoried based on fieldwork and the visual interpretation of satellite images. However, calculating the proportion of each island's land area covered by non-robust and robust geomorphic features occurring in island interiors was impossible for some islands due to the difficulty to discern the boundaries of these features on satellite imagery and to reach some inner island areas. We were therefore only able to generate qualitative data, i.e. to list these features and assess their overall significance (very high, high, moderate, low, undetectable) relative to island size, and rank it from 1 to 5 for each of the sample islands. Despite the absence of quantification limiting the robustness of the results on this variable, we consider that it is important to include it into the present assessment.

3.3.5. Variable 5: Island vegetation

Two major properties of atoll island vegetation influence island stability, namely (1) vegetation coverage, i.e. the proportion of an island's land area that is covered with vegetation, based on the assumption that island stability is proportional to vegetation coverage (Duvat and Pillet, 2017); (2) vegetation type, i.e. the respective proportions of native and introduced species, based on the assumption that native vegetation is more effective in trapping and stabilizing island sediments than introduced vegetation (Duvat et al., 2017b; Stoddart, 1963, 1971). Previous studies particularly highlighted that native coastal shrubs composed of *Scaevola taccada, Suriana maritima, Tournefortia argentea* and *Pemphis acidula* were more resistant and resilient to storm waves compared to introduced tree species

such as *Casuarina equisetifolia* and *Cocos nucifera* (Duvat et al., 2016; Duvat et al., 2017b; Duvat et al., 2020b; Stoddart, 1963, 1965; Woodroffe, 1983). Additionally, the presence of a dense and native coastal vegetation belt reduces wave penetration inland during storm events (Duvat et al., 2020b).

Vegetation coverage was obtained using the pan-sharpening images of 50 cm spatial resolution which were generated by the fusion between the multispectral and the panchromatic images. The Normalized Difference Vegetation index (NDVI; Tucker, 1979) was generated on each pan-sharpening image. KMEANS classifications and masks (Tou and Gonzalez, 1974) were performed to eliminate the non-vegetation and reef flat vegetation pixels. Five classes of vegetation coverage were distinguished: $x < 20\%$ (class 1); $20 \leq x < 40\%$ (class 2); $40 \leq x < 60\%$ (class 3); $60 \leq x < 80\%$ (class 4); $x \geq 80\%$ (class 5), with island physical robustness being proportional to vegetation coverage, i.e. low for class 1 vs. high for class 5.

The vegetation coverage maps were used to identify vegetation type using ArcGIS software (version 10.5.1). A supervised classification with the maximum likelihood algorithm (Strahler, 1980) was applied, based on extensive species sampling conducted on the ground used, first, to identify species which were classified according to their type, and second, to validate the results obtained. Species were classified as native (*Guettarda speciosa, Tournefortia argentea, Scaevola taccada, Suriana maritima* and *Pemphis acidula*), introduced (*Casuarina equisetifolia*, *Cocos nucifera*), and others (i.e. herbaceous, water plants and undetermined). The results were tested using the Kappa index, which validated the findings (values of 0.74-0.88). We considered the proportion of native species using five classes: $x < 20\%$ (class 1); $20 \leq x < 40\%$ (class 2); $40 \leq x < 60\%$ (class 3); $60 \leq x < 80\%$ (class 4); $x \geq 80\%$ (class 5), with island physical robustness being proportional to the proportion of native species.

Finally, the scores obtained for vegetation coverage and proportion of native species were averaged to obtain the final score. Five classes were distinguished: $1.00 \leq x < 1.80$ (class 1); $1.80 \leq x < 2.60$ (class 2); $2.60 \leq x < 3.40$ (class 3); $3.40 \leq x < 4.20$ (class 4); $x \geq 4.20$ (class 5), with island physical robustness increasing from a score of 1 to a score of 5.

3.3.6. Variable 6: Local human disturbances to island dynamics and natural capacity to adjust to climate-ocean changes

This variable considers all types of developments, interventions and activities that disrupt atoll island dynamics (Chunting and Howorth, 2003; Yamano et al., 2007; Collen et al., 2009; Webb and Kench, 2010; Kench, 2012; Biribo and Woodroffe, 2013; Duvat, 2013; McLean and Kench, 2015; Aslam and Kench, 2017) and thereby weaken island physical robustness through (1) the physical destruction of the island or of a part of the island, and/or (2) the disruption of the natural processes that drive an island's capacity to naturally adjust to climate-ocean changes. These human disturbances mainly include land reclamation, mining, shoreline hardening, the obstruction of sediment transport pathways, the contraction of available coastal accommodation space for sediment deposition and the destruction of the native vegetation. Island physical robustness is inversely proportional to the extent of such local human disturbances.

With the exception of water pollution, local human disturbances were inventoried based on fieldwork and the visual interpretation of aerial images (see Duvat et al., 2017a and 2020a). We qualitatively assess the level of impact of these disturbances, using the following scale:

(1) very high: disturbances are diverse and occur along the entire shoreline, to such an extent that they inhibit natural processes and prevent natural island adjustment to climate-ocean changes;

(2) high: disturbances are diverse along the entire shoreline or a highly impacting disturbance (e.g. shoreline hardening, sediment extraction or a harbor) affects the ocean and/or lagoon shoreline;

(3) moderate: disturbances are localized and have moderate impact on island dynamics and capacity to adjust to climate-ocean changes (e.g. jetty);

(4) limited: disturbances have limited impact on island dynamics and capacity to adjust to climate-ocean changes because they are very localized (e.g. one sediment extraction area) or have limited effect (e.g. pontoon);

(5) undetectable: no human disturbance is observed.

We averaged the scores of the ocean and lagoon coasts to obtain the final score, and distinguished between five classes, with island physical robustness increasing from class 1 (very high local human disturbances) to class 5 (undetectable human disturbances).

Although it has limitations, this qualitative assessment is currently the only available option to assess the contribution of local human disturbances to the undermining of island physical robustness. Major data gaps preventing us from conducting a quantitative assessment include uncertainty on both the sediment volumes extracted from beaches and shallow lagoon waters and their implications on island stability, as well as the impact of human constructions on alongshore and cross shore sediment transport. Despite these limitations, given that human disturbances are widespread on the northern inhabited islands of the atoll and therefore significantly influence the geomorphic robustness of these islands, we decided to include this variable into the assessment.

3.3.7. Calculation of island physical robustness

Each of the six variables was ranked on a five-level scale, where ranks 5 and 1 respectively correspond to the highest and lowest physical robustness. The six rankings were summed up

without weighting to provide a final estimate of the relative (i.e., compared to other islands) robustness of each island to changing boundary conditions. The lack of understanding of atoll island dynamics, especially of how the variables considered in this study interact to drive island physical robustness, prevented us from assigning weights to these variables. As each of the variables used in this assessment ranges from 1 to 5, the final score ranges from 6 to 30. The final scores were converted into an index comprised between 0 (for a result equalling to 6) and 1 (for a result equalling to 30). Robustness is considered very low for $x < 0.20$, low for $0.20 \leq x < 0.40$, moderate for $0.40 \leq x < 0.60$, high for $0.60 \leq x < 0.80$, and very high for $x \geq 0.80$. The index of 'island relative physical robustness' ranks each sample island related to the others.

4. Results

4.1. Variable 1: Island size

The twelve study islands have land areas ranging from 0.69 ha for island No.7, which is a rim-perpendicular elongated islet that formed between 1966 and 2013, to 464.20 ha for island No.1, both of which are settled (Table 3). Islands Nos. 6 and 7 (inhabited) rank 1 ($x < 10$ ha), while islands Nos. 3 and 4 (inhabited) rank 2 ($10 \leq x < 50$ ha); islands Nos. 8 to 10 (inhabited) rank 3 ($50 \leq x < 100$ ha); islands Nos. 2, 5 (inhabited) and 11 (uninhabited) rank 4 ($100 \leq x < 200$ ha); and islands Nos.1 (inhabited) and 12 (uninhabited) rank 5 ($x \geq 200$ ha). This emphasizes the high variation of island size along the atoll rim and the fact that small (ranking 2) to very small (ranking 1) islands are settled despite their high physical susceptibility to climate-ocean changes.

Table 3. Variation of island size across study islands.

Island No.	Images used (day/month/year)	Status	Land area (Ha)	Score
1	16/10/2016	Inhabited	464.20	5

2	01/10/2013	Inhabited	135.71	4
3	01/10/2013	Inhabited	13.08	2
4	01/10/2013	Inhabited	12.02	2
5	01/10/2013	Inhabited	105.14	4
6	01/10/2013	Inhabited	6.72	1
7	01/10/2013	Inhabited	0.69	1
8	01/10/2013	Inhabited	82.20	3
9	01/10/2013	Inhabited	67.05	3
10	16/10/2016	Inhabited	58.20	3
11	16/10/2016	Uninhabited	165.40	4
12	20/02/2015	Uninhabited	205.90	5

4.2. Variable 2: Island elevation

The sample islands exhibit contrasts in terms of elevation ranking, with two islands (Nos.1 and 6) ranking 1, four islands (Nos. 2, 3, 5 and 7) ranking 2, four islands (Nos. 4, 8, 10 and 12) ranking 3, and two islands (Nos. 9 and 11) ranking 4 (Table 4 and Figure 4). Of note, some of the settled islands, including island No.2 which hosts the main village of Avatoru, the airport island (No5) which is inhabited, and a few small nearby islands (Nos. 3, 6 and 7), exhibit low elevation scores of 1 or 2. In contrast, two settled islands exhibit high scores, including islands Nos. 8 (Ohotu; ranking 3) and 9 (Tiputa; ranking 4). This latter island was the first island of the northern part of the atoll to be settled in the 19th century when the population of the atoll moved to where the passes are located for commercial purposes.

In addition, marked between-island differences in elevation characteristics are revealed by the five indicators used to assess island elevation, including (1) averaged island elevation, (2) maximum averaged ocean-side beach ridge elevation, (3) maximum averaged lagoon-side beach ridge elevation, (4) lowest averaged elevation, and (5) highest averaged elevation (Table 4; Figures 4, 5 and 6; Supplementary Material 4.1 and 4.2).

Averaged island elevation varies from 1.65 m (island No.1) to 2.46 m (island No.11), with two islands ranking 1 (Nos. 1 and 12), five islands (Nos. 2, 3, 5, 6 and 10) ranking 2, three islands (Nos. 4, 7 and 8) ranking 3, and two islands (Nos. 9 and 11) ranking 5 (Table 4 and Figure 4). Within-island variations are marked, with some islands exhibiting contrasting cross-island topographic profiles, e.g. island No.1 (6 topographic profiles, with values ranging

from 1.08 to 2.07 m), while others show more homogenous topographic profiles, e.g. island No.8 (5 topographic profiles, with values ranging from 2.01 to 2.20 m) (Supplementary Material 4.1).

Maximum averaged ocean-side beach ridge elevation exhibits contrasting values ranging from 3.41 m (island No.2, rank 1) to 6.27 m (island No.12, rank 5) (Table 4; Figure 4; Figures 5A, 5B and 5C). Ten islands, that is, all islands with the exception of islands Nos. 9 and 12, have values < 4.50 m. These islands would flood as a result of ocean beach ridge wave overtopping in the event of a 1983-type TC based on the 4.50 m threshold proposed by Pedreros et al. (2010) (Figures 5 and 6D). Within-island variations are high, with 4 transects out of 43 showing values < 3 m (on islands Nos.1, 2 and 5) and 6 transects having values > 5 m (on islands Nos.9 and 12; Supplementary Material 4.2). The high values reported on island No.9 are partly due to human reworking of the storm ridge, including waste disposal at the top of the ridge.

Likewise, the values obtained for the maximum averaged lagoon-side beach ridge elevation vary between and within islands (Table 4 and Figure 4). Averaged values range from 1.44 m (island No.6, rank 1) to 2.27 m (island No.10, rank 5), with lowest and highest values of 1.15 m (island No.2) and 2.47 m (island No.10), respectively (Supplementary Material 4.2). This means that all islands would flood as a result of lagoon beach ridge wave overtopping in the event of a 1983-type TC based on the 2.1 m threshold proposed by Damlamian and Kruger (2013) (Figure 5). While island No.10 systematically exhibits lagoon-side beach ridge elevation values > 2 m, the other islands (e.g. island No.5) exhibit a high proportion of values < 1.50 m (Supplementary Material 4.2).

The lowest averaged (between all of the transects of a given island) elevation surveyed in the inner part of islands ranges from <1 (e.g. 0.93 m and 0.96 m for islands Nos.1 and 12, respectively; rank 1) to nearly 2 m (1.89 m for island No.10; rank 5) (Table 4 and Figure 4),

with minimum values of 0.44 and 0.68 m (island No.1, transects 5 and 3, respectively) (Supplementary Material 4.1 and 4.2).

Likewise, the highest averaged elevation varies importantly, from 3.41 m for island No.2 (rank 1) to 6.99 m for island No.11 (rank 5), which has ~200 m-wide sand dunes on its lagoon side (Table 4; Figure 4; Figure 5D and 5E; Figures 6A and 6B). Extreme values range from 2.70 m (island No.2, transect 1) to 8.24 m (island No.11, transect 1). Sixteen transects out of 43, including all transects of islands Nos.11 and 12 (Figure 5) and three out of the four transects considered on island No.9, exhibit values > 5 m, while four transects have values < 3 m (Supplementary Material 4.1 and 4.2). This means that islands Nos.11 and 12 and to some extent island No.9 would be the only ones to have flood-proof areas (either coastal or inner, depending on islands) in the event of a 1983-type TC.

Together, these findings show contrasting between- and within-island elevations (Figure 4). Whereas most islands have a higher ocean vs. a lower lagoon side (e.g. island No.12, Figures 5A, 5B, 5C), one island (No.11) uncommonly exhibits elevated lagoon-side sand dunes (Figures 5D and 5E). Additionally, whilst some islands (e.g. Nos.8 and 10) show limited variations in elevation from one transect to another, others (e.g. islands Nos.1 and 12) exhibit high inner variations. Moreover, it is noteworthy that some islands (e.g. island No.1) have very low-lying interiors, including island No.11 (with a lowest point of 1.09 m for transect 2) which however exhibits elevated sand dunes. Likewise, some islands (e.g. island No.12) that exhibit high (> 6 m) ocean-side beach ridges have comparatively low (< 2 m) lagoon-side elevations. All together, these findings highlight that nearly all islands have low- to very-low-lying areas, even those exhibiting the highest elevation values and having sand dunes and/or elevated ocean-side beach ridges.

Table 4. Variation of island elevation across study islands.

Elevations are expressed in meter, using the hydrographic zero as a reference. Of note, available numerical modelling studies indicate that Avatoru Island, northern part of Rangiroa Atoll, floods at extreme water levels of 4.5 m and 2.1 m (above hydrographic zero) on its ocean and lagoon coasts, respectively (Pedreros et al., 2010).

Island number	Averaged island elevation		Maximum averaged ocean-side beach ridge elevation		Maximum averaged lagoon-side beach ridge elevation		Lowest averaged elevation in the inner part of the island		Highest averaged elevation		Final ranking	
	Value (m)	Ranking	Value (m)	Ranking	Value (m)	Ranking	Value (m)	Ranking	Value (m)	Ranking	Score	Ranking
1	1.65	1	3.74	1	1.92	3	0.93	1	3.74	1	7	1
2	1.85	2	3.41	1	1.68	2	1.38	3	3.41	1	9	2
3	1.83	2	3.53	1	1.63	2	1.64	4	3.53	1	10	2
4	2.04	3	3.79	1	1.93	3	1.76	5	3.79	1	13	3
5	1.93	2	3.50	1	2.12	4	1.41	3	3.50	1	11	2
6	1.99	2	3.56	1	1.44	1	1.47	3	3.56	1	8	1
7	2.02	3	4.10	2	1.74	2	1.42	3	4.10	1	11	2
8	2.07	3	3.91	1	2.02	4	1.65	4	3.90	1	13	3
9	2.41	5	4.79	3	1.84	3	1.61	4	4.80	2	17	4
10	1.94	2	4.33	2	2.27	5	1.89	5	4.33	2	16	3
11	2.46	5	3.51	1	1.99	4	1.41	3	6.99	5	18	4
12	1.75	1	6.27	5	1.77	2	0.96	1	6.27	4	13	3

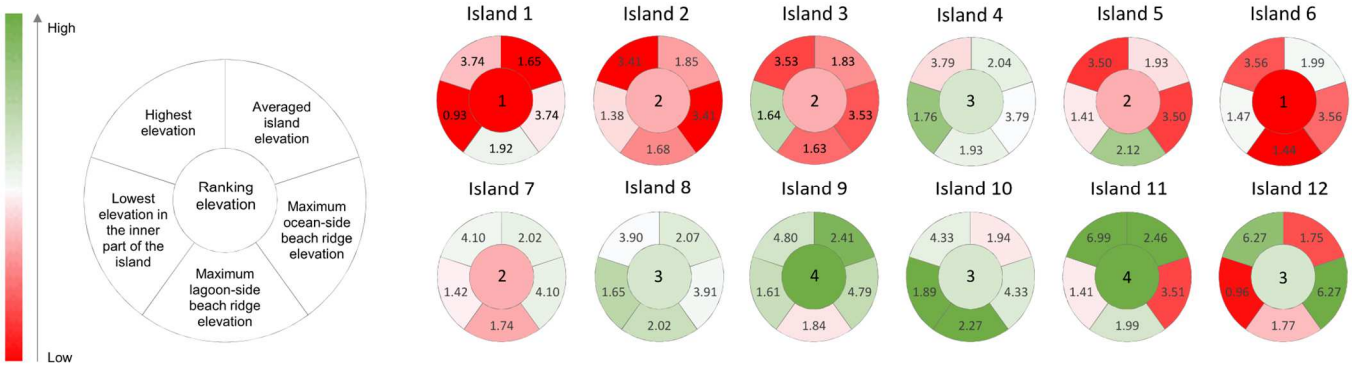

Figure 4. Between- and within-island variations of atoll island elevation.
For the five elevation criteria, values are indicated in meter. The final ranking, based on aggregated scores (see Table 4), is indicated in the center of diagrams. This figure highlights high between-island variations for all sub-criteria explaining scattered (ranking from 1 to 4) final elevation scores.

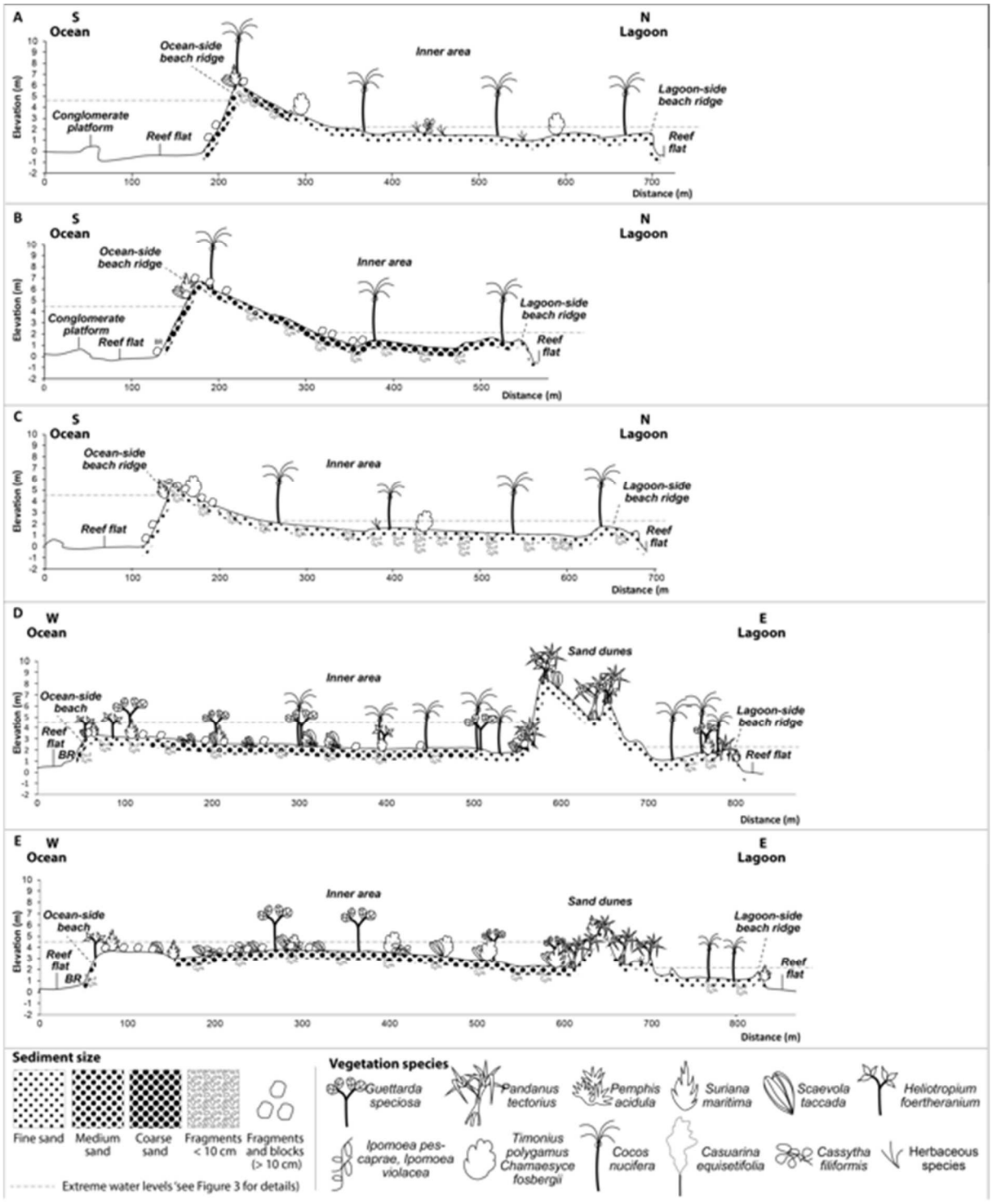

Figure 5. Topographic transects showing variations in island elevation, structure and vegetation.

Panels A, B and C respectively show transects 1, 3 and 5 of island No.12, while panels D and E show transects 2 and 7 of island No.11 (see Supplementary Material 2 for transect location). Island No.12 presents a typical atoll island profile, with a high ocean-side beach ridge and a low-lying lagoon

shoreline. Transects 2 (panel D) and 7 (panel E) on island No.11 highlight the low-lying nature of the ocean-side of the island where it corresponds to ancient hoa. In addition, this island uncommonly has elevated sand dunes stretching along its lagoon coast. In this figure, we show extreme water levels, assuming that they would reach similar levels on these islands as those reached on Avatoru Island (No.2 in Figure 2).

Figure 6. Geomorphic and ecological characteristics of Rangiroa Atoll islands.

Panels A and B show the high sand dunes stretching along the lagoon coast of island No.11. Panel C shows a storm rampart on the ocean coast of island No.1. Panel D provides an overview of the elevated (around 6 m above hydrographic zero) ocean coast of island No.12. Panels A, B and C show contrasts in vegetation type between island No.11, which mainly has native vegetation as shown in panels A and B, and cultivated islands (No.12), where introduced species such as coconut trees are predominant (Panel D).

4.3. Variable 3: Island shape

Island shape is variable (Figure 2), as highlighted by circularity indices ranging from 0.41 (rank 3) for island No.12 (a large and elongated boomerang-type island) to 0.83 (rank 5) for island No.6 (a small round island) (Table 5). Most small (<15 ha) islands have values ≥ 0.75 and rank 4, while the largest islands (> 100 ha), which stretch along the atoll rim, have values ≤ 0.61, and rank 3.

Table 5. Variation of island shape across study islands.

See section 3.3.3 for details on the method used to calculate island shape.

Island number	Island perimeter (m)	Island area (m^2)	Circularity index	Ranking
1	15,125.29	4,641,695.55	0.50	3
2	7,087.96	1,357,100.28	0.58	3
3	1,714,80	130,778.96	0.75	4
4	1,646.79	120,184.17	0.75	4
5	7,833.20	1,051,375.10	0.46	3
6	1,100.38	67,171.16	0.83	5
7	564.36	6,873.31	0.52	3
8	6,285.63	822,004.45	0.51	3
9	4,776.98	670,545.36	0.61	4
10	4,932.06	582,154.33	0.55	3
11	7,430.95	1,653,784.51	0.61	4
12	12,318.14	2,059,163.07	0.41	3

4.4. Variable 4: Island structure

Sample islands exhibit contrasting scores ranging from 3 to 5 as regards their structure (Table 6). Two islands (Nos. 1 and 11) rank 3. These islands have a terminal sand and gravel spit oriented in the direction of the alongshore drift on their lagoon side, extensive shore-parallel swamps along their lagoon-facing shoreline, and shore-perpendicular swamps and very low-lying areas stretching from ocean to lagoon corresponding to ancient hoa (Figure 2). Three islands rank 4, which exhibit inner swamps (island No.2), across-island low-lying areas corresponding to ancient hoa (island No.12) or both of these features (island No.5) (Figure 2). The other islands, where no non-robust geomorphic feature was detected, therefore rank 5.

Table 6. Variation of island structure across study islands.

See section 3.3.4 for details on the method used to assess island structure.

Island number	Type(s) of non-robust geomorphic feature	Overall significance related to the island land area	Ranking
1	Elongated lagoon-side swamps, inner swamps, ancient hoa, sand and gravel spit	Moderate	3
2	Inner swamps	Low	4
3	/	Very low	5
4	/	Very low	5
5	Ancient hoa, inner swamp	Low	4
6	/	Very low	5
7	/	Very low	5
8	/	Very low	5
9	/	Very low	5
10	/	Very low	5
11	Lagoon-side swamps, sand spits, very low-lying southern end, sand spit, ancient hoa	Moderate	3
12	Ancient hoa	Low	4

4.5. Variable 5: Island vegetation

Vegetation coverage varies from 38.56% for island No.7 to 74.13% for island No.12 (Table 7; Supplementary Material 5). Whereas one single island (i.e. recently-formed island No.7) exhibits a score of 2 (vegetation coverage < 40%), four islands have a score of 4 (vegetation coverage comprised between 40 and 60%) and seven islands a score of 4 (vegetation coverage comprised between 60 and 80%) (Table 7). Of note, some of the most densely populated islands experience a high vegetation coverage, such as islands Nos.2 (60.07%) and 9 (72.99%) that host the two main villages of the atoll.

Between-island contrasts are even more striking when considering vegetation type (Table 7 and Figure 7). The proportion of native species ranges from 11.67% for island No.3 to 65.64% for island No.11 (Supplementary Material 5; Figures 6A and 6B). Whereas five islands (Nos.2, 3, 5, 8 and 9) rank 1 with scores <20%, four islands (Nos. 1, 4, 7 and 10) rank 2 with scores comprised between 20 and 40%, two islands (Nos. 6 and 12) rank 3 with scores comprised between 40 and 60%, and one single island (island No.11) ranks 4 with a score of 65.64%. These findings reflect the high level of degradation of the native vegetation on both settled (i.e. islands Nos. 1 to 10, having a proportion of native species ranging from 11.67 to 41.90%) and cultivated islands (island No.12; 46.46%; Figure 6D), while the uninhabited and non-cultivated island considered in this study (island No.11) exhibits a much higher

proportion of native species (65.64%). On the former islands, the proportion of introduced vegetation is generally high, ranging from 39.53% (island No.9) to 62.41% (island No.8), except for island No.5 (25.90%) which hosts the atoll's airport and is mainly (i.e. over 57.00% of its surface) covered by herbaceous species.

Table 7. Variation in vegetation coverage and type across study islands.

Island No.	Vegetation coverage		Vegetation type (%)				Final vegetation score (and ranking)
	%	Score	Native	Introduced	Others	Score	
Island 1	64.45	4	31.54	52.37	16.09	2	3.00 (3)
Island 2	60.07	4	12.46	52.54	35.00	1	2.50 (2)
Island 3	44.48	3	11.66	52.83	35.51	1	2.00 (2)
Island 4	41.48	3	22.81	43.13	34.06	2	2.50 (2)
Island 5	42.40	3	17.13	25.90	56.97	1	2.00 (2)
Island 6	65.32	4	41.91	49.31	8.78	3	3.50 (4)
Island 7	38.56	2	36.39	61.17	2.44	2	2.00 (2)
Island 8	50.49	3	17.24	62.41	20.35	1	2.00 (2)
Island 9	72.99	4	11.82	39.53	48.65	1	2.50 (2)
Island 10	63.98	4	25.93	41.05	33.02	2	3.00 (3)
Island 11	70.33	4	65.64	24.10	10.26	4	4.00 (4)
Island 12	74.13	4	46.46	49.58	3.96	3	3.50 (4)

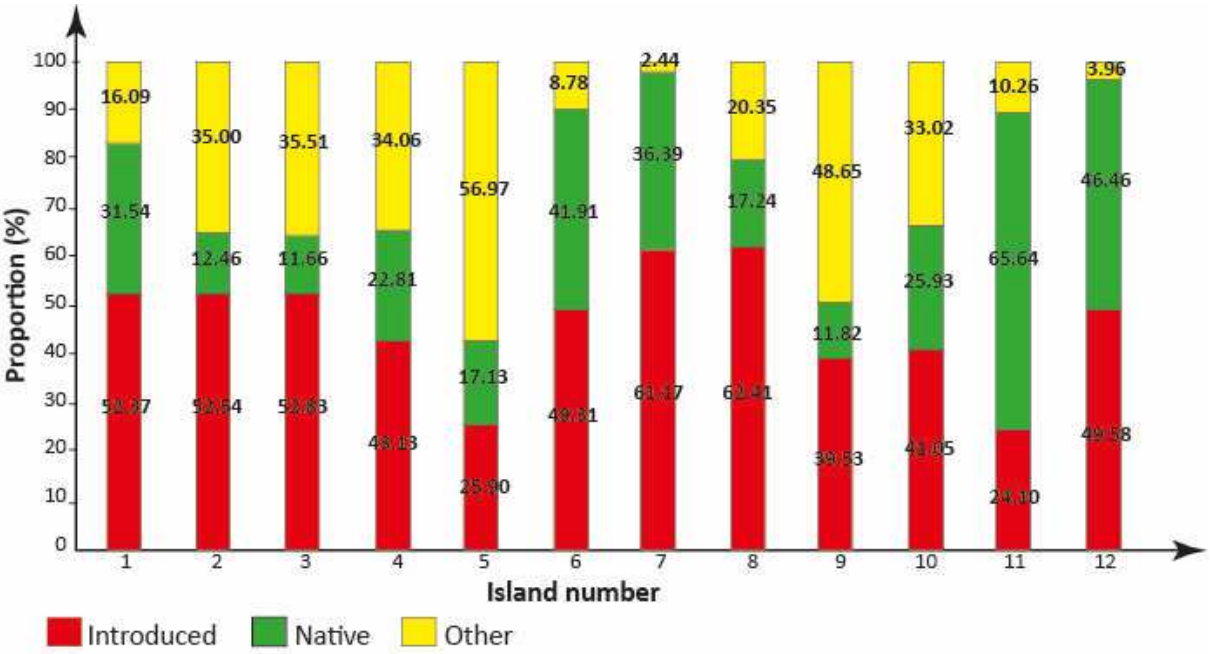

Figure 7. Variation of vegetation type across study islands.

Whereas introduced vegetation prevails on some of the settled islands (e.g. Nos. 7 and 8), native vegetation is predominant on some remote uninhabited islands (Nos. 11 and 12). Other vegetation includes in particular herbaceous species, which are dominant on the airport island (No.5).

Final vegetation scores (averaging of the scores obtained for vegetation coverage and proportion of native species) confirm that most islands exhibit low physical robustness from a vegetation perspective: seven islands (Nos.2, 3, 4, 5, 7, 8 and 9) rank 2, whereas two islands (Nos. 1 and 10) rank 3 and three islands (Nos.6, 11 and 12) rank 4 (Table 7 and Figure 7).

The findings finally allow defining three island types with regard to vegetation cover. Type 1 corresponds to settled islands, which exhibit a high proportion (>40% for all islands, except for island No.5) of introduced vegetation and a low proportion of native vegetation (<30% for 7 islands out of 10 and comprised between 30 and 42% for 3 islands), with other vegetation including secondary herbaceous species representing a high percentage of the total vegetation in some cases (e.g. island No.5, with ~57%). Type 2 corresponds to cultivated islands, which show a high proportion of both introduced (i.e. coconut groves) and native vegetation, as illustrated by island No.12 where these two categories respectively represent 49.58 and 46.46% of the island's vegetation. Type 3, illustrated by island No.11, corresponds to islands that are currently unsettled and non-cultivated but that have been cultivated in the past. Island No.11 predominantly has native (65.64%), followed by introduced (mostly coconut trees, 24.10%) and other vegetation (10.26%) corresponding to plants growing in lagoon-side swamps. Collectively, these findings highlight the high degradation of the vegetation coverage on most study islands.

4.6. Variable 6: Local human disturbances compromising island capacity to adjust to climate-ocean changes

The qualitative assessment of local human disturbances shows high between-island contrasts, with study islands ranking from 1 for densely populated islands (Nos. 2 to 9) to 5 for remote cultivated (No.12) and non-cultivated (No.11) islands exhibiting no or limited human

influence on shoreline dynamics (see details in Supplementary Material 6). Islands can be classified into three classes. The first one corresponds to densely populated islands (Nos.2 to 9) exhibiting extensive ocean-side sediment mining and the disruption of lagoon-side sediment production and deposition by sediment extraction (mostly from shallow lagoon waters), land reclamation and shoreline armoring, which rank 1. The second class corresponds to peri-urban islands (Nos. 1 and 10) exhibiting lower population densities and limited local human disturbances, consisting mainly of localized sediment dredging from reef flat and/or beaches, shoreline armoring and coastal structures (e.g. groins) locally disturbing cross-shore and alongshore sediment transport, which rank 2 (island No.10) or 3 (island No.1). The third and last class corresponds to remote uninhabited islands (Nos. 11 and 12) that currently are or previously were cultivated (i.e. have coconut groves) but exhibit no (e.g. island No.11) or very localized coastal developments (e.g. one jetty and dredged harbor basin for island No.12), which rank 5.

4.7. Contrasting levels of island physical robustness

The aggregation of the results obtained for each of the six abovementioned variables shows that study islands exhibit contrasting levels of relative physical robustness, with indices ranging from 0.33 for island No.7 to 0.75 for islands Nos.11 and 12 (Figure 8 and Supplementary Material 7). While nine islands out of twelve (representing 75% of the sample islands) exhibit a moderate relative physical robustness (index comprised between 0.40 and 0.60), one island (8.30%) experiences a low relative physical robustness (island No.7; index comprised between 0.20 and 0.40) and two islands (16.7%) a high relative physical robustness (islands Nos.11 and 12; index comprised between 0.60 and 0.80).

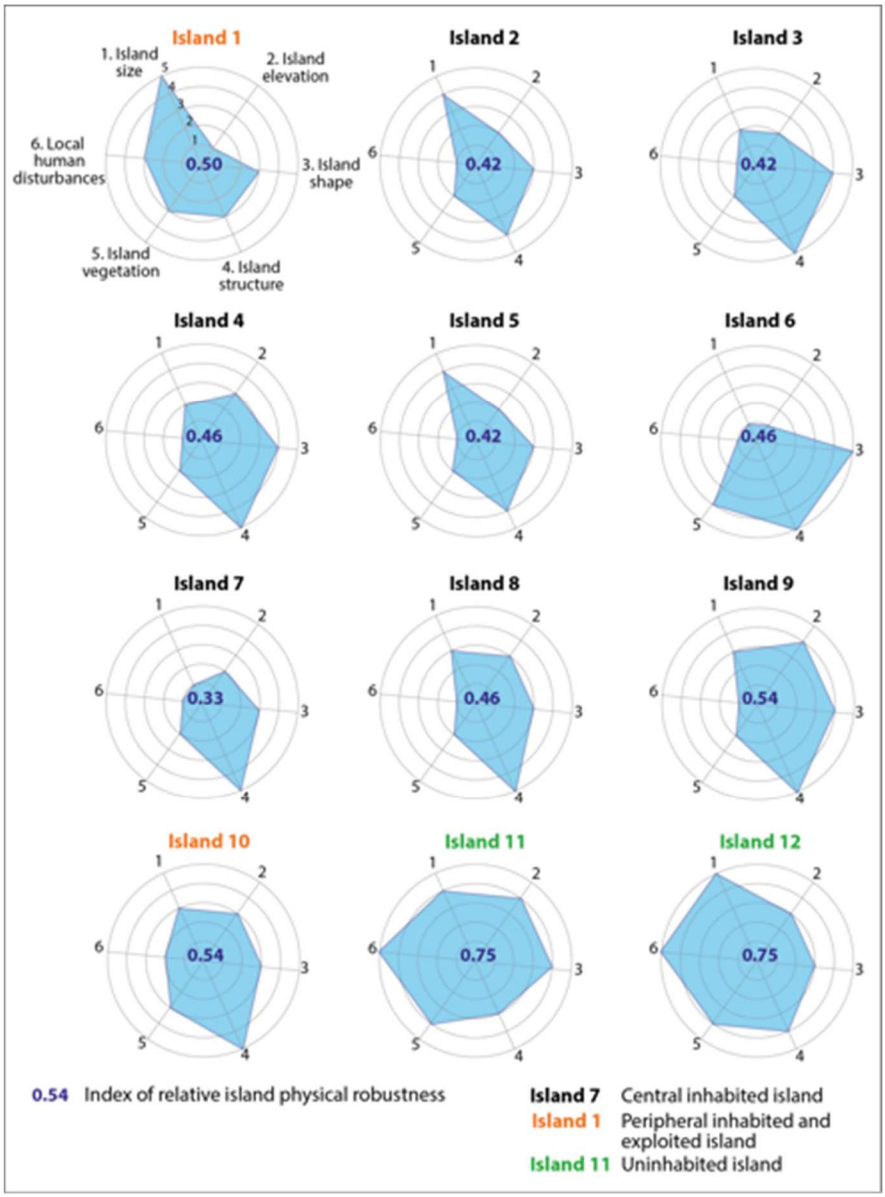

Figure 8. Contrasts in atoll island physical robustness.

Marked contrasts in atoll island physical robustness are shown by indices ranging from 0.33 to 0.75.

The main contributors to differences in island relative physical robustness are, in order of importance, (1) island size (variable 1), and local human disturbances to island dynamics and natural capacity to adjust to climate-ocean changes (variable 6), which exhibit values ranging from 1 to 5; (2) island elevation (variable 2), with values ranging from 1 to 4; and (3) island shape (variable 3), structure (variable 4), vegetation (variable 5), showing values ranging

across three levels on the 5-point scale used in this study, respectively from levels 3 to 5, 3 to 5, and 2 to 4.

5. Discussion

Using the example of Rangiroa Atoll, this study reveals that atoll islands exhibit contrasting levels of physical robustness, with some unsettled agricultural islands showing higher levels of physical robustness than the settled islands. This is, firstly, because inhabited islands were settled for economic reasons (proximity to passes allowing the promotion of commercial activities) regardless of their physical characteristics; and secondly, because local human activities have reduced the physical robustness of these islands over time through environmental degradation (removal of native vegetation, destruction of protective coastal features such as beach/storm ridges through sediment extraction or reworking). The peripheral rural and remote islands targeted for future development are large, have extensive relatively elevated (>3-4m) areas, and are for some of them (especially island No.12) less exposed to tropical cyclones compared to settled islands due to their location.

These findings suggest that within-atoll relocation of people and human assets is a relevant adaptation option for this (and probably other) atoll (s) by 2050 (under all climate scenarios) and potentially 2100 (at least under scenario RCP2.6; see Duvat et al., 2021 for detailed data on the exposure of the Central Pacific to climate change-related drivers). On Rangiroa Atoll and other atolls exhibiting such contrasting indices of physical robustness across their islands, within-atoll relocation of people and human assets could consist in moving the latter (1) from the less robust (i.e. unstable and flood-prone) toward the most robust (stable and elevated) areas within already settled islands, and (2) from the least robust (e.g. islands Nos. 2, 3, 5 and 7 in this study) to the most robust (e.g. islands Nos. 11 and 12) islands. This solution should be considered before more extreme solutions to climate change, such as migration to high

islands (especially Tahiti in this case), are considered. Importantly, this study shows that variations in island elevation are one among other factors to be considered to determine which island areas and islands are the most suitable for current-to-future human occupancy on atolls. Other physical (island size, island shape and island structure) and ecological (island vegetation, including vegetation coverage and proportion of native species that contribute to island stabilization) factors should also be fully considered.

On Rangiroa and other Tuamotu atolls, relocating people and human assets in more robust island areas and islands seems all the more relevant at the scale of the next decades to century that these islands are generally less exposed to flooding and its cascading impacts on livelihoods and economic activities than some other atoll islands worldwide (e.g. Fogafale, Funafuti Atoll, Tuvalu; Yamano et al., 2007). This is due to the combination of relatively low rates of SLR (2.5 mm ± 0.5 mm/y between 1950 and 2009), moderate subsidence (Ballu et al., 2011; Ballu et al., 2019) and very rare extensive (including cyclone-induced) island flooding (Duvat et al., 2018; Magnan et al., 2018). Furthermore, water and food security are expected to increase in the settled Tuamotu atolls, as a result of the equipment of all households with rainwater tanks by 2022 with the financial support of the French Government (with rainfall not projected to decrease under climate change in the Central Pacific; IPCC, 2019; Duvat et al., 2021) and the projected increase in tuna and tuna-like species in the Central Pacific (Duvat et al., 2021).

Beyond island elevation, the contribution of other drivers – including island size, structure, shape, vegetation and the degree of disturbance of island adjustment capacity by local human activities – to differences in island physical robustness emphasizes the need to include these variables in atoll island assessments, which in turn calls for data generation on these poorly known dimensions. No or very limited data exist on island vegetation, structure and disruption by local human activities. For instance, whilst local human disturbances are

acknowledged to alter urban island dynamics (see e.g. Duvat et al., 2020a and Yamano et al., 2007), most studies considering these disturbances focused on land reclamation and disregarded other disturbances. Yet, local human disturbances are diverse (twenty disturbances occurring in intertidal, coastal and inner land areas were recently listed by Duvat et al., 2020a) and have cumulative disruptive effects on atoll island dynamics and natural capacity to adjust to climate-ocean changes. Likewise, both the vegetation coverage and vegetation type (native vs. introduced) of atoll islands remains little documented despite the major role of vegetation attributes in island physical stability (especially response to storm events) and susceptibility to flooding. Given the variability of atoll island characteristics and physical robustness, filling these data gaps would also allow modelling studies (e.g. flood modelling) to make progress through both the inclusion of more variables and the running of models for different types of islands instead of one single and specific island (e.g. Storlazzi et al., 2018; Giardino et al., 2018).

Additionally, methodological barriers remain, which require further research efforts. The first barrier concerns the weighting of variables, which we considered equal in this study as a result of a lack of knowledge on their respective influence. Are some variables more influent than others in determining an atoll island's physical robustness? Does the degree of influence of variables vary according to contexts? The second methodological challenge relates to the determination of classes for each variable considered in such assessments. As a result of the paucity of data on atoll islands, we were not able to use 'standard' (i.e. relevant for atoll islands on the whole) minimum and maximum values to determine classes. We therefore used the minimum and maximum values generated for the study islands, which may not be relevant for other atoll islands. Filling the abovementioned data gaps and improving the understanding of the drivers and processes controlling atoll island physical robustness would help overcoming these two methodological gaps. This would also allow applying the

methodological framework used in this study to other atoll islands worldwide, and thereby determine the representativeness of the twelve islands considered in this study.

6. Conclusions

Atoll islands exhibit extremely diverse physical and human features, which together influence their current and future habitability. Recognizing that these islands are geomorphologically diverse, this article proposes a comprehensive assessment of their physical robustness that considers not only geomorphic, but also ecological and human determinants of this robustness.

Study islands exhibit contrasting levels of physical robustness, both at the variable scale and at the aggregated index scale. The main contributors to differences in island relative physical robustness are, in order of importance, (1) island size (variable 1), and local human disturbances (variable 6); (2) island elevation (variable 2); and (3) island shape (variable 3), structure (variable 4), and vegetation (variable 5). The aggregation of results into a physical robustness index shows that study islands exhibit contrasting levels of relative physical robustness, with indices ranging from 0.33 to 0.75. Whereas nine islands out of twelve (75% of the sample islands) exhibit a moderate relative physical robustness (index comprised between 0.40 and 0.60), one island (8.30%) experiences a low relative physical robustness (index comprised between 0.20 and 0.40) and two islands (16.7%) a high relative physical robustness (index comprised between 0.60 and 0.80).

Based on these results, we firstly advocate for more comprehensive assessments of atoll island physical robustness under climate change. Such assessments should indeed consider not only their elevation but also their size, shape and structure, as well as their ecological and human characteristics that also influence their change and susceptibility to physical (through shoreline erosion and marine flooding) destabilization. Our findings therefore highlight the need for increased research efforts on the under-researched dimensions of atoll island physical

robustness, including island vegetation and structure and the influence of human activities on atoll island capacity to adjust to climate-ocean changes. Such efforts will in turn pave the way to improved modelling of future risks threatening atoll islands. Second, at the scale of Rangiroa Atoll, this study emphasizes that some peripheral rural and remote islands that are targeted by the public authorities for future development have a much higher physical robustness than the settled islands. This finding makes within-atoll relocation of people and human assets to more robust island areas and islands a relevant adaptation strategy for this atoll and potentially other atolls worldwide, based on the assumption that atoll islands are also physically diverse elsewhere. However, such a strategy would only make sense if human disturbances, which are acknowledged to undermine atoll island physical robustness in many settings (Duvat and Magnan, 2019; Duvat et al., 2020a), were maintained at a low level on receiving islands in the future.

Acknowledgements

This work was supported by the Agence Nationale de la Recherche (France) under the STORISK research project (grant No. ANR-15-CE03-0003).

References

Albert, S., Leon, J. X., Grinham, A. R., Church, J. A., Gibbes, B. R., Woodroffe, C. D., 2016. Interactions between sea-level rise and wave exposure on reef island dynamics in the Solomon Islands. Environ. Res. Lett., 11(5), 054011. https://doi.org/10.1088/1748-9326/11/5/054011

Andrefouët, S., Chagnaud, N., Chauvin, C., Kranenburg, C.J., 2008. Atlas des récifs coralliens de France Outre-Mer. Centre IRD de Nouméa, Nouvelle-Calédonie, pp. 153 pp.

Andrefouët, A., Ardhuin, F., Queffeulou, P., Legendre, R., 2012. Island shadow effects and the wave climate of the Western Tuamotu Archipelago (French Polynesia) inferred from altimetry and numerical model data. Mar. Pollut. Bull. 65, 415–424. http://doi.org/10.1016/j.marpolbul.2012.05.042

Aslam, M., Kench, P.S., 2017. Reef island dynamics and mechanisms of change in Huvadhoo Atoll, Republic of the Maldives, Indian Ocean. Anthropocene 18, 57– 68. doi:http://dx.doi.org/10.1016/j.ancene.2017.05.003.

Ballu, V., Bouin, M.-N., Siméoni, P., Crawford, W.C., Calmant, S., Boré, J.-M., Kanas, T., Pelletier, B., 2011. Comparing the role of absolute sea-level rise and vertical tectonic motions in coastal flooding, Torres Islands, PNAS 108(32), 13019-22. https://doi.org/10.1073/pnas/1102842108

Ballu, V., Gravelle, M., Woppelmann, G., de Viron, O., Rebischung, P., Becker, M., Sakic, P., 2019. Vertical land motion in the Southwest and Central Pacific from available GNSS solutions and implications for relative sea levels. Geophys. J. Int. 218 (3), 1537-1551. http://doi.org/10.1093/gji/ggz247

Beetham, E., Kench, P. S., Popinet, S., 2017. Future Reef Growth Can Mitigate Physical Impacts of Sea-Level Rise on Atoll Islands. Earth's Future *5* (10), 1002-1014. https://doi.org/10.1002/2017ef000589.

Beetham, E., Kench, P.S., 2018. Predicting wave overtopping thresholds on coral reef-island shorelines with future sea-level rise. Nat.Commun., 9, 3997. https://doi.org/10.1038/s41467-018-06550

Bindoff, N.L., Cheung, W.W.L., Kairo, J.G., Arístegui, J., Guinder, V.A., Hallberg, … Williamson, P., 2019. *Changing Ocean, Marine Ecosystems, and Dependent Communities*. In: Pörtner, H.-O., Roberts, D.C., Masson-Delmotte, V., Zhai, P., Tignor, M., Poloczanska

E. et al. (Eds.), IPCC Special Report on the Ocean and Cryosphere in a Changing Climate. Geneva, Switzerland: World Meteorological Organization. https://www.ipcc.ch/site/assets/uploads/sites/3/2019/11/09_SROCC_Ch05_FINAL-1.pdf

Biribo, N., Woodroffe, C.D., 2013. Historical area and shoreline change of reef islands around Tarawa Atoll, Kiribati. Sustain Sci 8,345–362. https://doi.org/10.1007/s11625-013-0210-z

Canavesio, R., 2019. Distant swells and their impacts on atolls and tropical coastlines. The example of submersions produced by lagoon water filling and flushing currents in French Polynesia during 1996 and 2011 mega swells. Global Planet Change 177, 116-126. https://doi.org/10.1016/j.gloplacha.2019.03.018

Church, J.A., White, N.J., 2011. Sea-level rise from the late 19th to the early 21st century. Surv. Geophys. 32, 585–602. http://dx.doi.org/10.1007/s10712-011-9119-1.

Chunting, X., Howorth, R., 2003. Natural and artificial connections between atoll islets in the Pacific, their process and environmental impact. Journal of Ocean University of Qingdao 2(2), 195-200.

Collen, J.D., Garton, D.W., Gardner, J.P.A., 2009. Shoreline changes and sediment redistribution at Palmyra Atoll (Equatorial Pacific Ocean): 1874-Present. J Coast Res 253,711–722. https://doi.org/10.2112/08-1007.1

Cornwall, C.E., Comeau, S., Kornder, N.A., Perry, C.T., van Hooidonk, R., DeCarlo, T.M., Pratchett, M.S., Anderson, K.D., Browne, N., Carpenter, R., Diaz-Pulido, G., D'Olivo, J.P., Doo, S.S., Figueiredo, J., Fortunato, S.A.V., Kennedy, E., Lantz, C.A., McCulloch, M.T., González-Rivero, M., Schoepf, V., Smithers, S.G., Lowe, R.J., 2021. Global declines in coral reef calcium carbonate production under ocean acidification and warming. P NAS 118(21), e20152651118. https://doi.org/10.1013/pnas.20152651118

Damlamian, H., Kruger, J., 2013. 2D coupled hydrodynamic specttral wave model of Rangiroa. The 1983 Orama-Nisha Tropical Cyclone. SPC Applied Geoscience and Technology Division (SOPAC), Ocean and Islands Programme, 44 p.

Des Garets E., 2005. Bilan des connaissances sur les surcotes marines en Polynésie. Rapport BRGM/RP-55038-FR, 57 p.

Duvat, V., 2013. Coastal protection structures in Tarawa Atoll, Republic of Kiribati. Sustain. Sci. 8, 363–370. http://dx.doi.org/10.1007/s11625-013-0205-9

Duvat, V.K.E., 2019. A global assessment of atoll island planform changes over the past decades. Wiley Interdiscip. Rev. Clim. Change 10, e557. https://doi.org/10.1002/wcc.557.

Duvat, V.K.E., Magnan A.K., 2019. Rapid human-driven undermining of atoll island capacity to adjust to ocean climate-related pressures. Sci. Rep. 9, 15129. https://doi.org/10.1038/s41598-019-51468-3

Duvat V., Magnan A., Canavesio R., 2018. La variabilité des impacts des cyclones dans les atolls des Tuamotu (Polynésie Française), La Houille Blanche 2, 13-21. https://doi.org/10.1051/lhb/2018016

Duvat V., Magnan A., Etienne S., Salmon C., Pignon-Mussaud C., 2016. Assessing the impacts of and resilience to Tropical Cyclone Bejisa, Reunion Island (Indian Ocean), Nat. Hazards 83, 601-640. https://doi.org/10.1007/s11069-016-2338-5

Duvat, V.K.E., Magnan, A.K., Perry C.T., Spencer T., Bell, J.D., Wabnitz, C., Webb, A.P., White, I., McInnes, K., Gattuso, J.-P., Graham, N.A.J., Nunn, P.D., Le Cozannet, G., 2021. Risks to future atoll habitability from climate-driven environmental changes. Wiley Interdiscip. Rev. Clim. Change e700. https://doi.org/wcc.700

Duvat V.K.E., Pillet V., 2017. Shoreline changes in reef islands of the Central Pacific: Takapoto Atoll, Northern Tuamotu, French Polynesia. Geomorphology 282, 96-118. https://doi.org/10.1016/j.geomorph.2017.01.002

Duvat, V.K.E., Pillet, V., Volto, N., Terorotua, H., Laurent V., 2020b. Contribution of moderate climate events to atoll island building (Fakarava Atoll, French Polynesia). Geomorphology 354, 107057. https://doi.org/10.1016/jgeomorph.2020.107057

Duvat VKE, Salvat B, Salmon C., 2017a. Drivers of shoreline change in French Pacific atoll reef islands. Global Planet Change 158, 134-154. doi: 10.1016/j.gloplacha.2017.09.016

Duvat, V.K.E., Stahl, L., Costa, S., Maquaire, O., & Magnan, A., 2020a. Taking control of human-induced destabilisation of atoll islands: lessons learnt from the Tuamotu Archipelago, French Polynesia. Sustain. Sci. 15, 569-586. https://10.1007/s11625-019-00722-8

Duvat, V.K.E., Volto, N., Salmon C., 2017b. Impacts of category 5 tropical cyclone Fantala (April 2016) on Farquhar Atoll, Seychelles Islands, Indian Ocean. Geomorphology 298, 41-62. https://doi.org/10.1016/j.geomorph.2017.09.022

Ellison, J.C., Mosley, A., Helman, M., 2017. Assessing atoll shoreline condition to guide community management. Ecol. Indic. 75:321–330. https://doi.org/10.1016/ j.ecolind.2016.12.031

Ford, M.R., Kench, P.S., 2014. Formation and adjustment of typhoon-impacted reef islands interpreted from remote imagery: Nadikdik Atoll, Marshall Islands. Geomorphology 214, 216-222. https://doi.org/ 10.1016/j.geomorph.2014.02.006

Garcin, M., Vendé-Leclerc, M., Maurizot, P., Le Cozannet, G., Robineau, B., Nicolae-Lerma, A., 2016. Lagoon islets as indicators of recent environmental changes in the South Pacific:

the New Caledonian example. Cont. Shelf Res. 122, 120-140. https://doi.org/10.1016/j.csr.2016.03.025

Gattuso, J.-P., Magnan, A., Billé, R., Cheung, W.W.L., Howes, E.L., Joos, F., … Turley, C., 2015. Contrasting Futures for Ocean and Society from Different Anthropogenic CO_2 Emissions Scenarios. Science, 349 (6243). https://doi.org/10.1126/science.aac4722

Giardino, A., Nederhoff, K., Vousdoukas, M., 2018. Coastal hazard risk assessment for small islands: assessing the impact of climate change and disaster reduction measures on Ebeye (Marshall Islands). Reg. Environ. Change 18 (8), 2237-2248. https://doi.org/10.1007/s10113-018-1353-3

Gischler, E., 2016. Guyot, atoll. In: Harff, J., Meschede, M., Petersen, S. & Thiede, J. (Eds), Encyclopedia of Marine Geosciences, Springer, Dordrecht, pp. 302-309. https://doi.org/10.1007/978-94-007-6238-1

Hay, C.C., Morrow, E., Kopp, R.E., Mitrovica, J.X., 2015. Probabilistic reanalysis of twentieth-century sea-level rise. Nature 517, 481–484. http://dx.doi.org/10.1038/ nature14093

Hoeke, R.H., Damlamian, H., Aucan, J., Wandres, M., 2021. Severe flooding in the atoll nations of Tuvalu and Kiribati triggered by a distant Tropical Cyclone Pam. Frontiers in Marine Science. Front. Mar. Sci. 7, 539646. https://doi.org/10.3389/fmars.2020.539646

Holdaway, A., Ford, M., 2019. Resolution and scale controls on the accuracy of atoll island shorelines interpreted from satellite imagery. Appl. Geomat. 11, 339-352. https://doi.org/10.1007/s12518-019-00266-7

IPCC, 2019. IPCC Special Report on the Ocean and Cryosphere in a Changing Climate. Pörtner, H.-O., Roberts, D.C., Masson-Delmotte, V., Zhai, P., Tignor, M., Poloczanska, E. et al. (Eds.). https://www.ipcc.ch/srocc/

ISPF (Institut Statistique de la Polynésie française), 2017. Statistical data of French Polynesia. http://www.ispf.pf/bases/Recensements/2017/Donnees_detaillees/Population.aspx

Kane, H.H., Fletcher, C.H., 2020. Rethinking reef island stability in relation to anthropogenic sea level rise. Earth's Future 8, e2020EF001525. https://doi.org/10.1029/2020EF001525

Kench, P.S., 2012. Compromising reef island shoreline dynamics: lega- cies of the engineering paradigm in the Maldives. In: Cooper, J.A.G., Pilkey, O.H. (Eds.), Pitfalls of shoreline stabilization: selected case studies. Springer Science + Business Media Dordrecht, Germany, pp 165–186. https://doi.org/10.1007/978-94-007-4123-2_11

Kench, P.S., McLean, R.F., 2004. Hydrodynamics and sediment transport fluxes of functional hoa in an Indian Ocean atoll. Earth Surf. Process. Landf. 29, 933–953. http:// dx.doi.org/10.1002/esp.1072.

Kumar, L., Eliot, I., Nunn, P.D., Stul, T., McLean, R., 2018. An indicative index of physical susceptibility of small islands to coastal erosion induced by climate change: an application to the Pacific islands, Geomatics, Nat. Hazards Risk 9(1), 691-702. https://doi.org/10.1080/19475705.2018.1455749

Laben C.A., Brower B.V., 2000. Process for enhancing the spatial resolution of multispectral imagery using pan-sharpening. Google Patents.

Larrue, S., Chiron, T., 2010. Les îles de Polynésie française face à l'aléa cyclonique. VertigO 10(3). URL: https://vertigo.revues.org/10558

Magnan, A.K., M. Garschagen, J.-P. Gattuso, J.E. Hay, N. Hilmi, E. Holland, F. Isla, G. Kofinas, I.J. Losada, J. Petzold, B. Ratter, T.Schuur, T. Tabe, and R. van de Wal, 2019. Cross-Chapter Box 9: Integrative Cross-Chapter Box on Low-Lying Islands and Coasts. In: Pörtner, H.-O., Roberts, D.C., Masson-Delmotte, V., Zhai, P., Tignor, M., Poloczanska, E.,

Mintenbeck, K., Alegría, A., Nicolai, M., Okem, A., Petzold, J., Rama, B., Weyer, N.M. (Eds), IPCC Special Report on the Ocean and Cryosphere in a Changing Climate https://www.ipcc.ch/site/assets/uploads/sites/3/2019/11/11_SROCC_CCB9-LLIC_FINAL.pdf

Magnan, A.K., Ranché, M., Duvat, V.K.E., Prenveille, A., Rubia, F., 2018. L'exposition des populations des atolls de Rangiroa et de Tikehau (Polynésie française) au risque de submersion marine. VertigO 18(3). URL: http://journals.openedition.org/vertigo/23607. https://doi.org/10.4000/vertigo.23607

Mann, T., Westphal, H., 2014. Assessing long-term changes in the beach width of reef islands based on temporally fragmented remote sensing data. Remote Sens. 6, 6961–6987. https://doi.org/10.3390/rs6086961.

Masselink, G., Lazarus, E.D., 2019. Defining coastal resilience. Water 11, 2587. https://doi.org/10.3390/w11122587

McLean, R.F., 2011. Atoll islands (motu). In: Hopley D. (Ed.), Encyclopedia of modern coral reefs: structures, form and process. Springer, Science+Business Media B.V., pp 47-51. https://doi.org/10.1007/978-90-481-2639-2

McLean, R.F., Kench, P. S., 2015. Destruction or persistence of coral atoll islands in the face of 20th and 21st century sea-level rise? Wiley Interdiscip. Rev. Clim. Change 6, 445-463. https://doi.org/10.1002/wcc.350

Mentaschi, L., Vousdoukas, M.I., Voukouvalas, E., Dosio, A., & Feyen, L., 2017. Global changes of extreme coastal wave energy fluxes triggered by intensified teleconnection patterns. Geophys. Res. Lett. 44, 2416-2426, https://doi.org/10.1002/2016GL072488.

Montaggioni L.F., Martin-Garin, B., Salvat, B., Aubanel, A., Pons-Branchu, E., Paterne, M., Richard, M., 2021. Coral conglomerate platforms as foundations for low-lying reef islands

in French Polynesia (central south Pacific): new insights into the timing and mode of formation. Mar. Geol. 437: 106500. https://doi.org/10.1016/j.margeo.2021.106500

Nurse, L.A., McLean, R.F., Agard, J., Briguglio, L.P., Duvat-Magnan, V., Pelesikoti, N., … Webb, A., 2014. Small islands. In: Barros, V.R., Field, C.B., Dokken, D.J., Mastrandrea, M.D., Mach, K.J., Bilir, T.E. et al. (Eds.), Climate Change 2014: Impacts, Adaptation, and Vulnerability. Part B: Regional Aspects Contribution of Working Group II to the Fifth Assessment Report of the Intergovernmental Panel on Climate Change. Cambridge University Press, Cambridge, pp.1613-1654.

Oppenheimer, M., Glavovic, B., Hinkel, J., Van De Wal, R., Magnan, A., Abd-Elgawad, … Sebesvari, Z., 2019. Sea Level Rise and Implications for Low Lying Islands, Coasts and Communities. In: Pörtner, H.-O., Roberts, D.C., Masson-Delmotte, V., Zhai, P., Tignor, M., Poloczanska, E. et al. (Eds.). IPCC Special Report on the Ocean and Cryosphere in a Changing Climate. Geneva, Switzerland: World Meteorological Organization. https://report.ipcc.ch/srocc/pdf/SROCC_FinalDraft_Chapter4.pdf

Owen, S.D., Kench, P. S., Ford, M., 2016. Improving understanding of the spatial dimensions of biophysical change in atoll island countries and implications for island communities: a Marshall Islands' case study. Appl. Geogr. 72, 55-64. https://doi.org/10.1016/j.apgeog.2016.05.004

Pedreros R., Krien Y., Poisson B., 2010. Programme ARAI 2. Caractérisation de la submersion marine liée aux houles cycloniques en Polynésie française. Rapport BRGM/RP58990-FR, pp. 64.

Perry, C.T., Alvarez-Filip, L., Graham, N.A.J., Mumby, P.J., Wilson, S.K., Kench, P.S., … Macdonald, C., 2018. Loss of coral reef growth capacity to track future increases in sea level. Nature 558(7710), 396. https://doi.org/10.1038/s41586-018-0194-z

Pirazzoli, P.A., Montaggioni, L.F., 1986. Late Holocene sea-level changes in the northwest Tuamotu islands, French Polynesia. Quat. Res. 25, 350–368. http://dx.doi.org/10.1016/0033-5894(86)9006-2.

Purkis, S.J., Gardiner, R., Johnston, M.W., Sheppard, C.R.C., 2016. A half-century of coastline change in Diego Garcia, the largest atoll island in the Chagos. Geomorphology 261, 282–298. https://doi.org/10.1016/j.geomorph.2016.03.010.

Richmond, R., 1992. Development of atoll islands in the Central Pacific. In: Proceedings of the 7th International Coral Reef Symposium, Guam. vol. 2. pp. 1185–1194.

Schuerch M., Spencer, T., Temmerman, S., Kirwan, M.L., Wolff, C., Lincke, D., … Brown, S., 2018. Future response of global coastal wetlands to sea-level rise. Nature 561, 231-234. https://doi.org/10.1038/s41586-018-0476-5

SHOM, 2016. Références Altimétriques Maritimes des ports de France métropolitaine et d'outre-mer, pp.116.

Shope, J. B., Storlazzi, C.D., Hoeke, R. K., 2017. Projected atoll shoreline and run-up changes in response to sea-level rise and varying large wave conditions at Wake and Midway Atolls, Northwestern Hawaiian Islands. Geomorphology 295, 537-550. https://doi.org/10.1016/j.geomorph.2017.08.002

Shope, J. B., Storlazzi, C.D., 2019. Assessing Morphologic Controls on Atoll Island Alongshore Sediment Transport Gradients Due to Future Sea-Level Rise. Front. Mar. Sci. 6. https://doi.org/10.3389/fmars.2019.00245.

Spennemann, D.H.R., 1996. Nontraditional settlement patterns and typhoon hazards on contemporary Majuro Atoll, Republic of the Marshall Islands. Environ. Manag. 20 (3), 337–348. https://doi.org/10.1007/BF01203842

Stoddart, D.R., 1963. Effects of hurricane Hattie on the British Honduras reefs and cays, October 30–31, 1961. Atoll Res. Bull. 95, 1–142.

Stoddart, D.R., 1965. Re-survey of hurricane effects on the British Honduras reefs and cays. Nature CCVII, pp. 589–592.

Stoddart, D.R., 1969. Reconnaissance geomorphology of Rangiroa Atoll, Tuamotu Archipelago. Atoll Res. Bull. 125, 71 pp.

Stoddart, D.R., 1971. Coral reefs and islands and catastrophic storms. In: Steers, J.A. (Ed.), Applied Coastal Geomorphology. Palgrave Macmillan, UK, pp. 155–197.

Stoddart, D.R., Steers, J.A., 1977. The nature and origin of coral reef islands. In: Jones, O.A., Endean, R. (Eds.), Biology and Geology of Coral Reefs. vol. 4, Geology no 2. Academic Press, New York, pp. 59–105.

Storlazzi, C.D., Gingerich, S.B., van Dongeren, A., Cheriton, O.M., Swarzenski, P.W., Quataert, E., Voss, C.I., … McCall, R., 2018. Most atolls will be uninhabitable by the mid-21st century because of sea-level rise exacerbating wave-driven flooding. Sci. Adv. 4 (4). https://doi.org/10.1126/sciadv.aap9741

Strahler, A. J., 1980. The use of prior probabilities in maximum likelihood classification of remotely sense data, Remote Sens. Environ. 10, 135-163.

Tou, J. T., Gonzalez, R. C., 1974. Pattern Recognition Principles, Addison-Wesley Publishing Company, Reading, Massachusetts.

Tuck, M., Kench, P.S., Ford, M.R., Masselink, G., 2019. Physical modelling of the response of reef islands to sea level rise. Geology 479, 803-806. https://doi.org/10.1130/G46362

Tucker, C.J., 1979. Red and photographic infrared linear combinations for monitoring vegetation. Remote Sens. Environ. 8, 127–150.

Vitousek, S., Barnard, P.L., Fletcher, C.H., Frazer, N., Erikson, L., & Storlazzi, C.D., 2017. Doubling of coastal flooding frequency within decades due to sea-level rise. Sci. Rep. 7(1), 1399. https://doi.org/10.1038/s41598-017-01362-7.

Webb, A., Kench, P.S., 2010. The dynamic response of reef islands to sea- level rise: evidence from multi-decadal analysis of island change in the central Pacific. Glob Planet Change 72, 234–246. https://doi.org/10.1016/j.gloplacha.2010.05.003

Woodroffe, C.D., 1983. The impact of cyclone Isaac on the coast of Tonga. Pacific Science 37(3), 181-210.

Woodroffe, C.D., 2008. Reef-island topography and the vulnerability of atolls to sea-level rise. Glob. Planet. Change 62, 77-96. https://doi.org/10.1016/j.gloplacha.2007.11.001

Yamano, H., Kayenne, H., Yamaguchi, T., Kuwahara, Y., Yokoki, H., Shimazaki, H., & Chikamori, M., 2007. Atoll island vulnerability to flooding and inundation revealed by historical reconstruction: Fongafale Islet, Funafuti Atoll, Tuvalu. Glob. Planet. Change *57*, 407–416. https://doi.org/10.1016/j.gloplacha.2007.02.007